Available online at www.sciencedirect.com
ScienceDirect
International Journal of Solids and Structures 45 (2008) 2251–2264
INTERNATIONAL JOURNAL OF SOLIDS AND STRUCTURES
www.elsevier.com/locate/ijsolstr

Free-edge stresses and progressive cracking in surface coatings of circular torsion bars

Xiang-Fa Wu [a,*], Yuris A. Dzenis [a], Kyle W. Strabala [b]

[a] *Department of Engineering Mechanics, Nebraska Center for Materials and Nanoscience, University of Nebraska-Lincoln, Lincoln, NE 68588-0526, USA*

[b] *Department of Mechanical Engineering and Department of Mathematics, University of Nebraska-Lincoln, Lincoln, NE 68588-0656, USA*

Received 13 July 2007; received in revised form 4 November 2007
Available online 8 December 2007

Abstract

This paper considers the explicit solutions of free-edge stresses near circumferential cracks in surface coatings of circular torsion bars and their application in determining the progressive cracking density in the coating layers. The problem was formulated within the framework of linear elastic fracture mechanics (LEFM). The free-edge stresses near crack tip and the shear stresses in the cross-section of the torsion bar were approached in explicit forms based on the variational principle of complementary strain energy. Criterion for progressive cracking in the coating layer was established in sense of strain energy conservation, and the crack density is thereby estimated. Effects of external torque, aspect ratio, and elastic properties on the density of progressive cracking were examined numerically. The present study shows that, in the sense of inducing a given crack density, compliant coating layer with lower modulus has much higher critical torque than that of a stiffer one with the same geometries and substrate material, i.e., compliant coating layer has greater cracking tolerance. Meanwhile, the study also indicates that thicker surface coating layer is more pliant to cracking than the thinner ones. The present model can be used for analyzing the damage mechanism and cracking tolerance of surface coatings of torsion shafts and for data reduction of torsional fracture test of brittle surface coatings, etc.

Keywords: Free-edge stress; Progressive cracking; Surface coatings; Torsional shaft bar; Fracture criterion; Energy release rate (ERR)

1. Introduction

Surface coatings have been used extensively in modern industries as anticorrosion coatings, solid lubricants, thermal barriers of gas turbines, and optical reflectors on organic glasses, among others. Typical surface coating system belongs to brittle thin-film on compliant substrate. Cracking and buckling delamination of the brittle coating layers may appear in surface coating layers under the action of planar strains that may be resulted from external loading, temperature change or even residual thermal stresses. In the past two decades, signif-

* Corresponding author. Tel.: +1 402 472 1680; fax: +1 402 472 8292.
E-mail address: xfwu@unlserve.unl.edu (X.-F. Wu).

0020-7683/$ - see front matter © 2007 Elsevier Ltd. All rights reserved.
doi:10.1016/j.ijsolstr.2007.11.020

icant progress has been made to understanding the cracking and buckling delamination in surface coating systems. Among those, the simplest theoretical delineation of cracking in surface coatings is based on Cox's shear-lag model (Cox, 1952). Recent detailed analysis of cracking and buckling delamination in flat surface-coating systems with multiple failure modes has been conducted (Hutchinson and Suo, 1992; Evans et al., 2001; Mishnaevsky and Gross, 2004, 2005; Xia and Hutchinson, 2000; Shenoy et al., 2001; Vlassak, 2003; Liang et al., 2004 and refs therein). When considering the mechanical behavior of surface coating layer on curved substrate (e.g., cylindrical surface), the substrate curvature may enhance or suppress the delamination, depending on the sign of the curvature and the direction of declamation growth (Hutchinson, 2001; Faulhaber et al., 2006). Based on the mixed-mode fracture theory of thin layers (Hutchinson and Suo, 1992; Suo and Hutchinson, 1990), delamination analysis indicated that, for thin elastic films bonded to cylindrical substrates and subjected to equi-biaxial compressive pre-stresses, the circumferential delamination growth is suppressed in the case of negative substrate curvature (interior surface); in contrast it is favored in the case of positive substrate curvature (exterior surface) (Hutchinson, 2001). It also showed that the axial growth of the delamination is independent of the radius of the cylindrical substrate. In addition, recent investigation of buckling delamination in compressed multilayers on curved substrates further explored the mechanisms of buckling delamination and spalling of surface coatings, and therefore provided feasible testing protocols in measuring their mechanical properties, e.g., the delamination toughness and stress distribution in the surface coating system (Faulhaber et al., 2006).

So far, a variety of special surface coatings have been developed such as those made of diamond-like carbon, annealed boron carbide, and amorphous Pb-Mo-S (Singer et al., 2003; Wang and Kato, 2003a,b; Donnet and Erdemir, 2004), which are capable of being employed as solid lubricants and anticorrosion coatings for power transmission shafts. In addition to their lower friction, these surface coating materials exhibit greater wear resistance and fracture toughness. In practice, when subjected to torsional loading, high shear stress in shift bars may induce cracking and delamination in these brittle coating layers. Circumferential cracking in surface coating layers may occur in some specific conditions when the crack growth is governed by shearing. As a matter of fact, there exist two competitive mechanisms to govern the growth of the cracking, i.e., the delamination growth along coating/substrate interface and the increase of the cracking density or the growth of cracks in the coating layers. The actual cracking mode depends upon the fracture toughness of the coating material, interface toughness, aspect ratio (ratio of the coating layer thickness to the radius of the circular shaft bar), and the elasticity dissimilarity of the coating layer and the substrate. Furthermore, for cracked surface coating layers, interfacial stresses near the crack tip can be treated as free-edge stresses which have been extensively studied in laminated composites since the pioneering work by Pipes and Pagano (Pipes and Pagano, 1970). Free-edge stress analysis in laminated composites has been reviewed in the recent literature (Mittelstedt and Becker, 2004a,b; Wu and Dzenis, 2005).

Nevertheless, to authors' knowledge, no model has been reported yet on the progressive cracking and the stress state of a circular torsion bar with multiple cracks in surface coatings. Therefore, in this work, we initiate the study in determining the free-edge stresses and the criterion of progressive cracking in cracked coating layer of a circular torsion bar. We limit our formulation within the framework of linear elastic fracture mechanics (LEFM). By assuming linear distribution of the shear stresses in the cross-section of the torsion bar, the free-edge stresses near crack tip of the coating layer and the entire shear stresses in the cross-section are determined through the variation of the complementary strain energy (Washizu, 1968; Hu, 1984). Criterion of progressive cracking and the resulting cracking density are established in the sense of strain energy conservation. Effects of the aspect ratio and the mechanical properties of the coating system on the free-edge stresses and the cracking density are examined numerically. Application of the present method is further addressed in the end of the paper.

2. Problem statement and solution

2.1. Governing equations

Consider a long cylindrical shaft bar with circular cross-section and uniform surface coating layer subjected to external torque T at two ends, as illustrated in Fig. 1. The shear moduli of the torsion bar and the coating

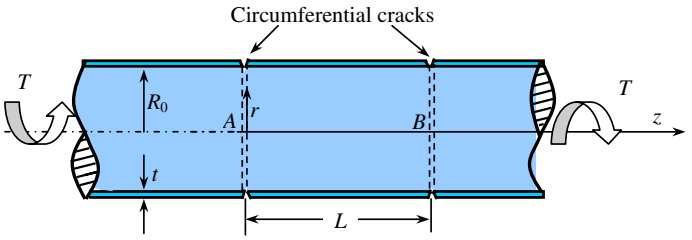

Fig. 1. Circumferential cracks in the surface coating layer of a circular torsion bar.

layer are assigned as G_1 and G_2, respectively. The radius of the torsion bar is denoted R_0, and the thickness of the coating layer is assigned as t. When subjected to sufficiently large torque T, cracking in the coating layer and/or delamination of the coating layer may appear. Hereafter, we only consider the simplest failure case, i.e., only periodic circumferential cracking appears in the coating layer. In such specific case, the cracking is governed by pure shearing. With the increase of the twisting load, the density of the circumferential cracks will increase monotonely.

Due to the axisymmetry of the system under consideration, a cylindrical (r,z)-coordinate system is introduced along the bar axis (Fig. 1). The deformations of the bar and the surface coating layer under consideration are pure shear. The nontrivial stresses are only two shear stresses, i.e., $\tau_{r\theta}(r,z)$ and $\tau_{\theta z}(r,z)$. Thus, the resulting equilibrium equation is (Timoshenko and Goodier, 1951)

$$\frac{1}{\rho^2}\frac{\partial}{\partial\rho}(\rho^2\tau_{r\theta})+\frac{\partial\tau_{\theta_z}}{\partial\xi}=0, \tag{1}$$

where ρ and ξ are two dimensionless coordinates such that $\rho=r/R_0$ and $\xi=z/R_0$. In the following, variables with subscript "1" are related to those of the torsion bar (substrate); while variables with subscript "2" are attached to those of the coating layer. As a matter of fact, the exact stress state will become complicated once circumferential cracking happens in the coating layer. To approach the stress distribution in the torsion bar with cracked coating layer, we use the principle of the minimum complementary strain energy (Washizu, 1968; Hu, 1984) based on the following stress assumption:

The stress components $\tau_{\theta z1}$ and $\tau_{\theta z2}$ in the torsion bar and the coating layer vary linearly with the coordinate ρ such that

$$\tau_{\theta z1}(\rho,\xi)=\rho\tau_1(\xi), \quad (0\leqslant\rho\leqslant 1) \tag{2}$$

$$\tau_{\theta_z 2}(\rho,\xi)=\rho\tau_2(\xi), \quad (1\leqslant\rho\leqslant 1+\eta,\ \eta=t/R_0) \tag{3}$$

where $\tau_1(\xi)$ and $\tau_2(\xi)$ are two unknown functions to be determined. Similar stress assumption has been used in approaching the shear stresses in tubular lap joints (Volkersen, 1965; Adams and Peppiatt, 1977; Chen and Cheng, 1992). When considering a typical torsion bar segment between two parallel circumferential cracks (see Fig. 1), the traction boundary conditions at $z=0$ and $z=L$ lead to

$$\tau_1(0)=\tau_1(\lambda)=\frac{2T}{\pi R_0^3}, \quad (\lambda=L/R_0) \tag{4}$$

$$\tau_2(0)=\tau_2(\lambda)=0. \tag{5}$$

The formal solutions for $\tau_{\rho\theta1}$ and $\tau_{\rho\theta2}$ can be determined by substituting (2) and (3) into Eq. (1) such that

$$\tau_{\rho\theta1}(\rho,\xi)=-\frac{\rho^2}{4}\frac{d\tau_1}{d\xi}, \quad (0\leqslant\rho\leqslant 1) \tag{6}$$

$$\tau_{\rho\theta2}(\rho,\xi)=\frac{(1+\eta)^4-\rho^4}{4\rho^2}\frac{d\tau_2}{d\xi}, \quad (1\leqslant\rho\leqslant 1+\eta). \tag{7}$$

Stress continuity at $\rho=1$, i.e., $\tau_{\rho\theta1}|_{\rho=1}=\tau_{\rho\theta2}|_{\rho=1}$, gives

$$\frac{d\tau_1}{d\xi} + [(1+\eta)^4 - 1]\frac{d\tau_2}{d\xi} = 0. \tag{8}$$

Integrating Eq. (8) with respect to the dimensionless variable ξ from 0 to arbitrary location ξ between 0 and λ leads to

$$\int_0^{\xi} d\tau_1 + [(1+\eta)^4 - 1]\int_0^{\xi} d\tau_2 = 0. \tag{9}$$

This relation can be further simplified by using the traction conditions (4) and (5) as

$$\tau_1(\xi) + [(1+\eta)^4 - 1]\tau_2(\xi) = \frac{2T}{\pi R_0^3}. \tag{10}$$

The governing equation in determining the unknown functions $\tau_1(\xi)$ and $\tau_2(\xi)$ can be formulated through the variational principle of the complementary strain energy (Washizu, 1968; Hu, 1984). In the present problem, the complementary strain energy of the torsion bar segment between 0 and λ consists of the contribution by both the torsion bar and the coating layer:

$$U = U_1 + U_2, \tag{11}$$

where

$$U_1 = \frac{R_0^3}{2G_1}\int_0^{\lambda}\int_0^{1}(\tau_{\rho\theta 1}^2 + \tau_{\theta_z 1}^2)2\pi\rho\, d\rho\, d\xi, \tag{12}$$

$$U_2 = \frac{R_0^3}{2G_2}\int_0^{\lambda}\int_1^{1+\eta}(\tau_{\rho\theta 2}^2 + \tau_{\theta_z 2}^2)2\pi\rho\, d\rho\, d\xi. \tag{13}$$

Substituting (2), (3), (6), and (7) into integrals (12) and (13) yields

$$U_1 = \frac{R_0^3}{2G_1}\int_0^{\lambda}\int_0^{1}\left\{\frac{\rho^4}{16}\left(\frac{d\tau_1}{d\xi}\right)^2 + \rho^2[\tau_1(\xi)]^2\right\}2\pi\rho d\rho d\xi = \frac{\pi R_0^3}{G_1}\int_0^{\lambda}\left\{\frac{1}{96}\left(\frac{d\tau_1}{d\xi}\right)^2 + \frac{1}{4}[\tau_1(\xi)]^2\right\}d\xi, \tag{14}$$

and

$$\begin{aligned} U_2 &= \frac{R_0^3}{2G_2}\int_0^{\lambda}\int_1^{1+\eta}\left\{\left[\frac{(1+\eta)^4 - \rho^4}{4\rho^2}\right]^2\left(\frac{d\tau_2}{d\xi}\right)^2 + \rho^2[\tau_2(\xi)]\right\}2\pi\rho\, d\rho\, d\xi \\ &= \frac{\pi R_0^3}{G_2}\int_0^{\lambda}\left\{\left\{\frac{(1+\eta)^8}{32}\left[1 - \frac{1}{(1+\eta)^2}\right] - \frac{(1+\eta)^4}{16}[(1+\eta)^2 - 1] + \frac{1}{96}[(1+\eta)^6 - 1]\right\}\right. \\ &\quad \left.\times\left(\frac{d\tau_2}{d\xi}\right)^2 + \frac{1}{4}[(1+\eta)^4 - 1][\tau_2(\xi)]^2\right\}d\xi. \end{aligned} \tag{15}$$

As a result, relations (14) and (15) can be rewritten as

$$U_1 = \frac{\pi R_0^3}{4G_1}\int_0^{\lambda}\left\{\frac{1}{24}\left(\frac{d\tau_1}{d\xi}\right)^2 + [\tau_1(\xi)]^2\right\}d\xi, \tag{16}$$

and

$$U_2 = \frac{\pi R_0^3}{4G_2}\int_0^{\lambda}\left\{A\left(\frac{d\tau_2}{d\xi}\right)^2 + \alpha[\tau_2(\xi)]^2\right\}d\xi, \tag{17}$$

where A and α are two coefficients related to the geometrical aspect ratio, i.e.

$$A = \frac{(1+\eta)^8}{8}\left[1 - \frac{1}{(1+\eta)^2}\right] - \frac{(1+\eta)^4}{4}[(1+\eta)^2 - 1] + \frac{1}{24}[(1+\eta)^6 - 1], \alpha = (1+\eta)^4 - 1. \tag{18}$$

For convenience in the following derivation, relation (10) is recast as

$$\tau_1(\xi) = \tau_0 - \alpha\tau_2(\xi), \tag{19}$$

where

$$\tau_0 = \frac{2T}{\pi R_0^3}. \tag{20}$$

Therefore, substituting (16), (17), and (20) into (11) leads to

$$U = \frac{\pi R_0^3}{4G_2}\int_0^{\lambda}\left\{(A+\alpha^2\beta/24)\left(\frac{\mathrm{d}\tau_2}{\mathrm{d}\xi}\right)^2 + \beta[\tau_0 - \alpha\tau_2(\xi)]^2 + \alpha[\tau_2(\xi)]^2\right\}\mathrm{d}\xi, \tag{21}$$

where β is the index of modulus dissimilarity defined by

$$\beta = G_2/G_1. \tag{22}$$

By applying the principle of minimum complementary strain energy (Washizu, 1968; Hu, 1984), functional (21) results in the governing differential equation:

$$(A+\alpha^2\beta/24)\frac{\mathrm{d}^2\tau_2}{\mathrm{d}\xi^2} - \alpha(1+\alpha\beta)\tau_2(\xi) + \alpha\beta\tau_0 = 0. \tag{23}$$

2.2. Two elementary solutions for shear stresses in circular torsion bars with circumferential cracks

The general solution to Eq. (23) can be expressed as

$$\tau_2(\xi) = C_1\exp(-k\xi) + C_2\exp[-k(\lambda-\xi)] + \frac{\beta\tau_0}{1+\alpha\beta}. \tag{24}$$

Here, k is the positive root of the characteristic equation resulted from Eq. (23):

$$k = \sqrt{\frac{\alpha(1+\alpha\beta)}{A+\alpha^2\beta/24}}, \tag{25}$$

and C_1 and C_2 are two coefficients that can be determined by the traction-free boundary condition (5), i.e.

$$C_1 = C_2 = -\frac{\beta\tau_0}{1+\alpha\beta}\frac{1}{1+\exp(-k\lambda)}. \tag{26}$$

Therefore, solution (24) can be expressed in explicit form such that

$$\tau_2(\xi) = \frac{\beta\tau_0}{1+\alpha\beta}\left\{1 - \frac{\cosh[k(\lambda/2-\xi)]}{\cosh(k\lambda/2)}\right\}. \tag{27}$$

Consequently, substitution of (10) and (27) into (2), (3), (6), and (7) gives the complete stress field in the circular torsion bar with circumferential cracks in the surface coating layer.

Here, we consider a limiting case of single circumferential crack at $\xi = 0$, and the corresponding traction conditions are

$$\tau_1(0) = \frac{2T}{\pi R_0^3}, \quad \tau_2(0) = 0, \tag{28}$$

$$\tau_1(\infty) + \alpha\tau_2(\infty) = \frac{2T}{\pi R_0^3}. \tag{29}$$

By determining the unknowns C_1 and C_2 in (24) to satisfy the traction conditions (28) and (29), the solution to single circumferential crack is

$$\tau_2(\xi) = \frac{\beta\tau_0}{1+\alpha\beta}[1 - \exp(-k\xi)]. \tag{30}$$

In the limiting case of $\xi \to +\infty$, relations (29) and (30) tend to the trivial crack-free solution:

$$\tau_1(+\infty) = \frac{\tau_0}{1+\alpha\beta}, \quad \tau_2(+\infty) = \frac{\beta\tau_0}{1+\alpha\beta}. \tag{31}$$

Moreover, by substituting (30) and (31) into (2), (3), (6), and (7), we obtain the stress field in a crack-free torsion bar with surface coatings:

$$\tau_{\rho\theta_1}(\rho) = 0, \quad \tau_{\theta_z 1}(\rho) = \frac{\rho\tau_0}{1+\alpha\beta}, \quad \tau_{\rho\theta_2}(\rho) = 0, \quad \tau_{\theta_z 2}(\rho) = \frac{\rho\beta\tau_0}{1+\alpha\beta}. \tag{32}$$

In the limiting case of homogenous circular torsion bar, i.e., $\beta = 1$, solution (32) recovers the stress field given by the elementary torsion bar theory. It should be mentioned that the actual free-edge stresses near crack tip are singular in view of LEFM and classic elasticity (wedge problem). The exact analytic expressions of the free-edge stresses are complicated and are hard to obtain when taking into account the interface and the finite dimensions. Therefore, the above approximate stress expressions provide an efficient engineering method for stress comparison and parameter analysis, similar to those developed for free-edge stress analysis of laminated composite materials (Pipes and Pagano, 1970; Mittelstedt and Becker, 2004a,b; Wu and Dzenis, 2005).

3. Progressive cracking analysis

3.1. Critical torque T_c for first circumferential cracking in surface coating layers of circular torsion bars

Within the framework of LEFM, the cracking criterion is that, subjected to the constant torque T_c, the strain energy increase ΔU due to cracking is equal to the strain energy release $\Delta\Gamma$ such that

$$\Delta U = \Delta\Gamma = \pi G_c[(1+\eta)^2 - 1]R_0^2, \tag{33}$$

where G_c is the critical energy release rate (ERR) of the circumferential crack in the coating layer. In this case, the circumferential cracking belongs to mode-II type since the crack initiates at some point and then grows under in-plane pure shear. Similar energy scheme has been used in determining the critical tensile stress in inducing progressive matrix cracking in laminated polymer composites (Laws and Dvorak, 1988). Therefore, by using the strain energy integral (21) and solutions (30) and (31), the increase of strain energy due to first circumferential cracking can be determined as

$$\begin{aligned}\Delta U &= \frac{\pi R_0^3}{2G_2}\int_0^{+\infty}\left\{(A+\alpha^2\beta/24)\left(\frac{\mathrm{d}\tau_2}{\mathrm{d}\xi}\right)^2 + \beta[\tau_0 - \alpha\tau_2(\xi)]^2 + \alpha[\tau_2(\xi)]^2\right\}\mathrm{d}\xi \\ &\quad - \frac{\pi R_0^3}{2G_2}\int_0^{+\infty}\left\{\beta[\tau_0 - \alpha\tau_2(+\infty)]^2 + \alpha[\tau_2(+\infty)]^2\right\}\mathrm{d}\xi, \\ &= \frac{\pi R_0^3}{4G_2}\left(\frac{\beta\tau_0}{1+\alpha\beta}\right)^2\left[(A+\alpha^2\beta/24)k + \frac{\alpha(1+\alpha\beta)}{k}\right].\end{aligned} \tag{34}$$

Substituting (34) into (33) determines the corresponding critical torque:

$$T_c = \left(\frac{\beta}{1+\alpha\beta}\right)^{-1}\sqrt{\frac{(1+\eta)^2-1}{(A+\alpha^2\beta/24)k + \alpha(1+\alpha\beta)/k}}\sqrt{G_2 G_c}(\pi R_0^{5/2}). \tag{35}$$

It should be claimed that the solution given above is resulted from the assumption of complete circumferential cracking. In order to evaluate the above method, we also consider the ERR of a single circumferential crack in the limiting case that the coating layer and the substrate have the same material properties. Calculation shows that the relationship between the ERR and the aspect ratio has the growth tendency very close to that predicted by the exact asymptotical method (Benthem and Koitor, 1973), and the deviation is relatively small for a wide range of the aspect ratio.

3.2. Progressive circumferential cracking and crack density in surface coating layers of circular torsion bars

In an attempt to study the progressive cracking in surface coating layer of a circular torsion bar, it is desirable to determine the density of circumferential cracks as a function of the external torque. Therefore, consider the case that the external torque gradually increases its magnitude till it reaches the critical value T_c, at which the next circumferential crack appears between two adjacent cracks with spacing L (see Fig. 2). It is reasonable to first consider the next crack at an arbitrary locus C between AB. Based on the strain energy criterion (33), it reads

$$\begin{aligned}\pi G_c[(1+\eta)^2-1]R_0^2 = \frac{\pi R_0^3}{4G_2}\Bigg\{&\int_0^{\lambda_1}\left\{(A+\alpha^2\beta/24)\left(\frac{d\tau_2}{d\xi}\right)^2+\beta[\tau_0-\alpha\tau_2(\xi)]^2+\alpha[\tau_2(\xi)]^2\right\}d\xi\\ &+\int_0^{\lambda_2}\left\{(A+\alpha^2\beta/24)\left(\frac{d\tau_2}{d\xi}\right)^2+\beta[\tau_0-\alpha\tau_2(\xi)]^2+\alpha[\tau_2(\xi)]^2\right\}d\xi\\ &-\int_0^{\lambda}\left\{(A+\alpha^2\beta/24)\left(\frac{d\tau_2}{d\xi}\right)^2+\beta[\tau_0-\alpha\tau_2(\xi)]^2+\alpha[\tau_2(\xi)]^2\right\}d\xi\Bigg\},\end{aligned} \tag{36}$$

where $\lambda_1 = L_1/R_0$, $\lambda_2 = L_2/R_0$, $\lambda = L/R_0$ ($\lambda = \lambda_1 + \lambda_2$), and $\tau_2(\xi)$ is given by (27) with the variable λ corresponding to the individual integration domain. The three integrals in (36) can be expressed explicitly. As a result, relation (36) can be rewritten as

$$\pi G_c[(1+\eta)^2-1]R_0^2 = \frac{\pi R_0^3}{8G_2}\left(\frac{\beta\tau_0}{1+\alpha\beta}\right)^2(D_1+D_2-D), \tag{37}$$

where

$$\begin{aligned}D_1 = &\frac{1}{k\cosh^2(k\lambda_1/2)}\{k\lambda_1[1/(\alpha^2\beta)+(2-Ak^2+(1-k^2)\alpha^2\beta)\\ &+(1+1/\alpha^2\beta)\cosh(k\lambda_1)]+[1+Ak^2+(1+k^2/24)\alpha^2\beta]\sinh(k\lambda_1)\},\end{aligned} \tag{38}$$

$$\begin{aligned}D_2 = &\frac{1}{k\cosh^2(k\lambda_2/2)}\{k\lambda_2[1/(\alpha^2\beta)+(2-Ak^2+(1-k^2)\alpha^2\beta)\\ &+(1+1/\alpha^2\beta)\cosh(k\lambda_2)]+[1+Ak^2+(1+k^2/24)\alpha^2\beta]\sinh(k\lambda_2)\},\end{aligned} \tag{39}$$

$$\begin{aligned}D = &\frac{1}{k\cosh^2(k\lambda/2)}\{k\lambda[1/(\alpha^2\beta)+(2-Ak^2+(1-k^2)\alpha^2\beta)\\ &+(1+1/\alpha^2\beta)\cosh(k\lambda)]+[1+Ak^2+(1+k^2/24)\alpha^2\beta]\sinh(k\lambda)\}.\end{aligned} \tag{40}$$

Consequently, the resulting critical torque T_c can be extracted from (37) such that

$$T_c = \sqrt{2}\left(\frac{\beta}{1+\alpha\beta}\right)^{-1}\sqrt{\frac{(1+\eta)^2-1}{D_1+D_2-D}}\sqrt{G_2G_c}(\pi R_0^{5/2}). \tag{41}$$

Without loss of generality, the locus C of next crack can be assumed as a random variable. Here we introduce the probability density function p that describes the site of the next circumferential crack. As a result, the ex-

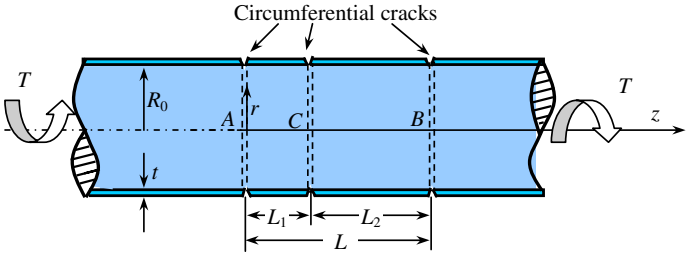

Fig. 2. An arbitrary circumferential crack between two adjacent cracks.

pected value of the external critical torque in inducing the next circumferential crack in the circular torsion bar which already contains cracks of the dimensionless cracking density $d(=1/\lambda)$ is

$$E[T_c(d)] = \int_0^{\lambda} p(\xi) T_c(\xi)\, d\xi, \tag{42}$$

where $T_c(\xi)$ is given by (41). The choice of the probability density function is crucial. Here we consider three candidates similar to those discussed in progressive matrix cracking in cross-ply polymer composite laminates (Laws and Dvorak, 1988).

The first case assumes an extreme situation that the next circumferential cracking would be guaranteed to occur at the exact mid-point of the unbroken portion of the surface coating layer, which is corresponding to the minimum torque for the next cracking. In this case, the corresponding density function p is the Dirac delta function, i.e.

$$p(\xi) = \delta(\xi - \lambda/2). \tag{43}$$

The second case considers another extreme situation that the next circumferential cracking is assumed to be possible equally as

$$p(\xi) = 1/\lambda. \tag{44}$$

The last more appealing hypothesis is to assume that $p(\xi)$ be proportional to the shear stress given by (27) such that

$$p(\xi) = \frac{1}{\lambda}\left\{1 - \frac{\cosh[k(\lambda/2 - \xi)]}{\cosh(k\lambda/2)}\right\}\left[1 - \frac{\tanh(k\lambda/2)}{k\lambda/2)}\right]^{-1}, \tag{45}$$

which favors the simple linear fracture mechanics.

Therefore, in the case of distribution (43), the expected critical torque can be expressed in explicit form by substituting (41) and (43) into (42) as

$$E[T_c(\lambda)] = \sqrt{2}\left(\frac{\beta}{1+\alpha\beta}\right)^{-1}\sqrt{\frac{(1+\eta)^2 - 1}{D_1 + D_2 - D}}\sqrt{G_2 G_c}(\pi R_0^{5/2}), \tag{46}$$

where D_1, D_2, and D are defined in (38)–(40) with $\lambda_1 = \lambda_2 = \lambda/2$. However, numerical scheme has to be employed in determining the expected critical torque T_c in the cases of (44) and (45) as demonstrated in Section 4.2 below.

4. Numerical examples

4.1. Free-edge stresses in circular torsion bars with cracked surface coatings

Closed-form solutions for shear stresses in a circular torsion bar with circumferentially cracked surface coating layer can be determined by plugging (19), (27), and (30) into (2), (3), (6), and (7). As a result, the shear stress field in a circular torsion bar with single circumferential crack is

$$\tau_{\theta z1}(\rho, \xi) = \frac{\rho\tau_0}{1+\alpha^2\beta}[1 + \alpha^2\beta\exp(-k\xi)], \quad (0 \leqslant \rho \leqslant 1) \tag{47}$$

$$\tau_{\rho\theta 1}(\rho, \xi) = \frac{\rho^2}{4}\frac{k\alpha^2\beta\tau_0}{1+\alpha^2\beta}\exp(-k\xi), \quad (0 \leqslant \rho \leqslant 1) \tag{48}$$

$$\tau_{\theta z2}(\rho, \xi) = \frac{\rho\alpha\beta\tau_0}{1+\alpha^2\beta}[1 - \exp(-k\xi)], \quad (1 \leqslant \rho \leqslant 1+\eta, \eta = t/R_0) \tag{49}$$

$$\tau_{\rho\theta 2}(\rho, \xi) = \frac{(1+\eta)^4 - \rho^4}{4\rho^2}\frac{k\alpha\beta\tau_0}{1+\alpha^2\beta}\exp(-k\xi), \quad (1 \leqslant \rho \leqslant 1+\eta). \tag{50}$$

Correspondingly, the shear stress field in a circular torsion bar with periodic circumferential cracks of spacing λ is

$$\tau_{\theta z1}(\rho,\xi)=\frac{\rho\tau_0}{1+\alpha^2\beta}\left\{1+\alpha^2\beta\frac{\cosh[k(\lambda/2-\xi)]}{\cosh(k\lambda/2)}\right\},\quad(0\leqslant\rho\leqslant1) \tag{51}$$

$$\tau_{\rho\theta1}(\rho,\xi)=\frac{\rho^2}{4}\frac{k\alpha^2\beta\tau_0}{1+\alpha^2\beta}\frac{\sinh[k(\lambda/2-\xi)]}{\cosh(k\lambda/2)},\quad(0\leqslant\rho\leqslant1) \tag{52}$$

$$\tau_{\theta z2}(\rho,\xi)=\rho\frac{\alpha\beta\tau_0}{1+\alpha^2\beta}\left\{1-\frac{\cosh[k(\lambda/2-\xi)]}{\cosh(k\lambda/2)}\right\},\quad(1\leqslant\rho\leqslant1+\eta,\eta=t/R_0) \tag{53}$$

$$\tau_{\rho\theta2}(\rho,\xi)=\frac{(1+\eta)^4-\rho^4}{4\rho^2}\frac{k\alpha\beta\tau_0}{1+\alpha^2\beta}\frac{\sinh[k(\lambda/2-\xi)]}{\cosh(k\lambda/2)},\quad(1\leqslant\rho\leqslant1+\eta). \tag{54}$$

To illustrate the effects of aspect ratio and modulus dissimilarity on the shear stress distribution, we plot the variations of the dimensionless shear stress $\tau_{\theta z2}(1,\xi)/\tau_0$ and the interfacial circumferential shear stress $\tau_{\rho\theta2}(1,\xi)/\tau_0$ in the coating layer vs. the dimensionless distance $\xi(\xi=x/R_0)$ from the crack tip for varying aspect ratio $\eta=t/R_0$ and index of modulus dissimilarity $\beta=G_2/G_1$, respectively, as shown in Figs. 3–5. In

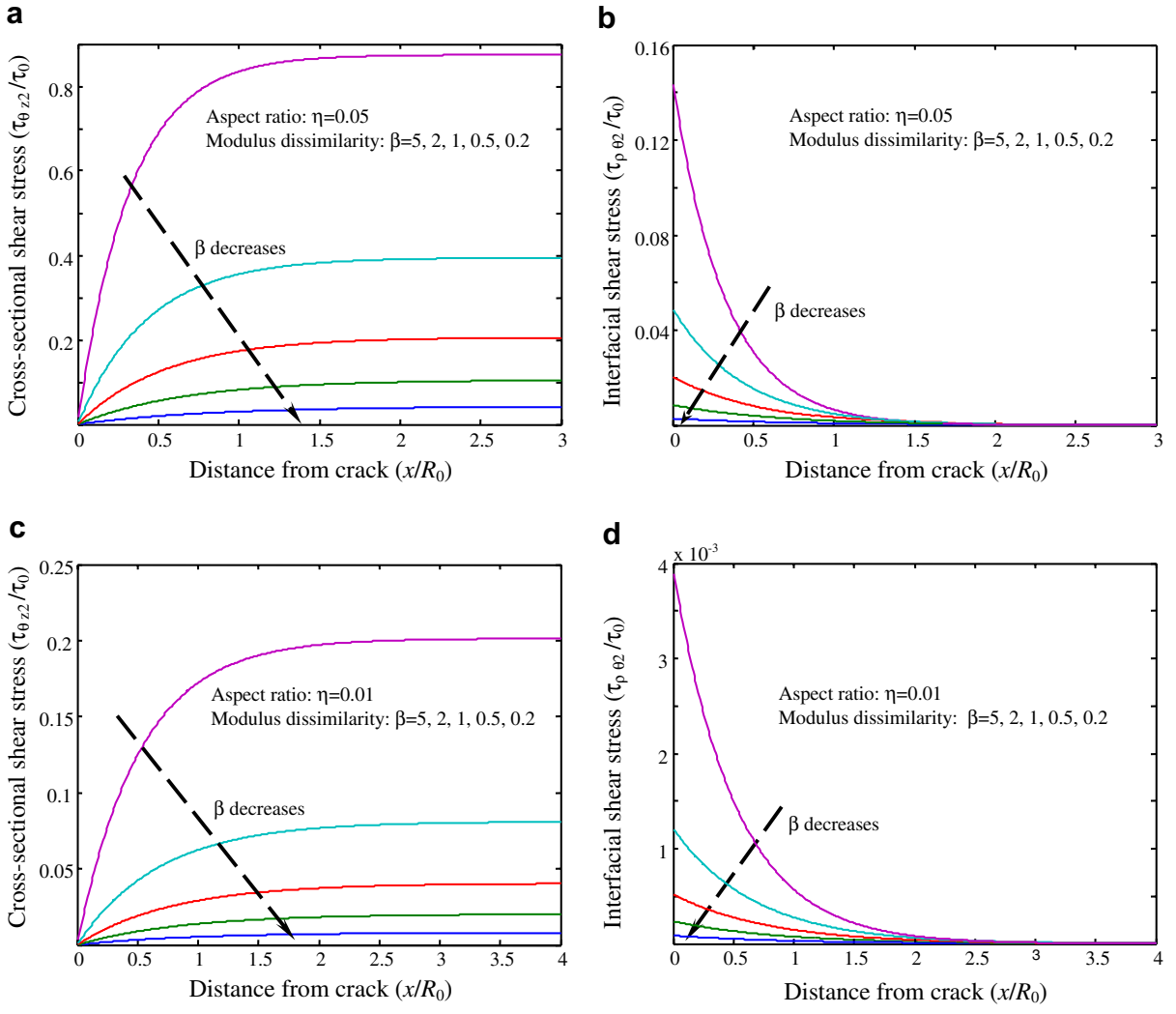

Fig. 3. Interfacial free-edge shear stresses for single circumferential cracking in the surface coating layer of a circular torsion bar.

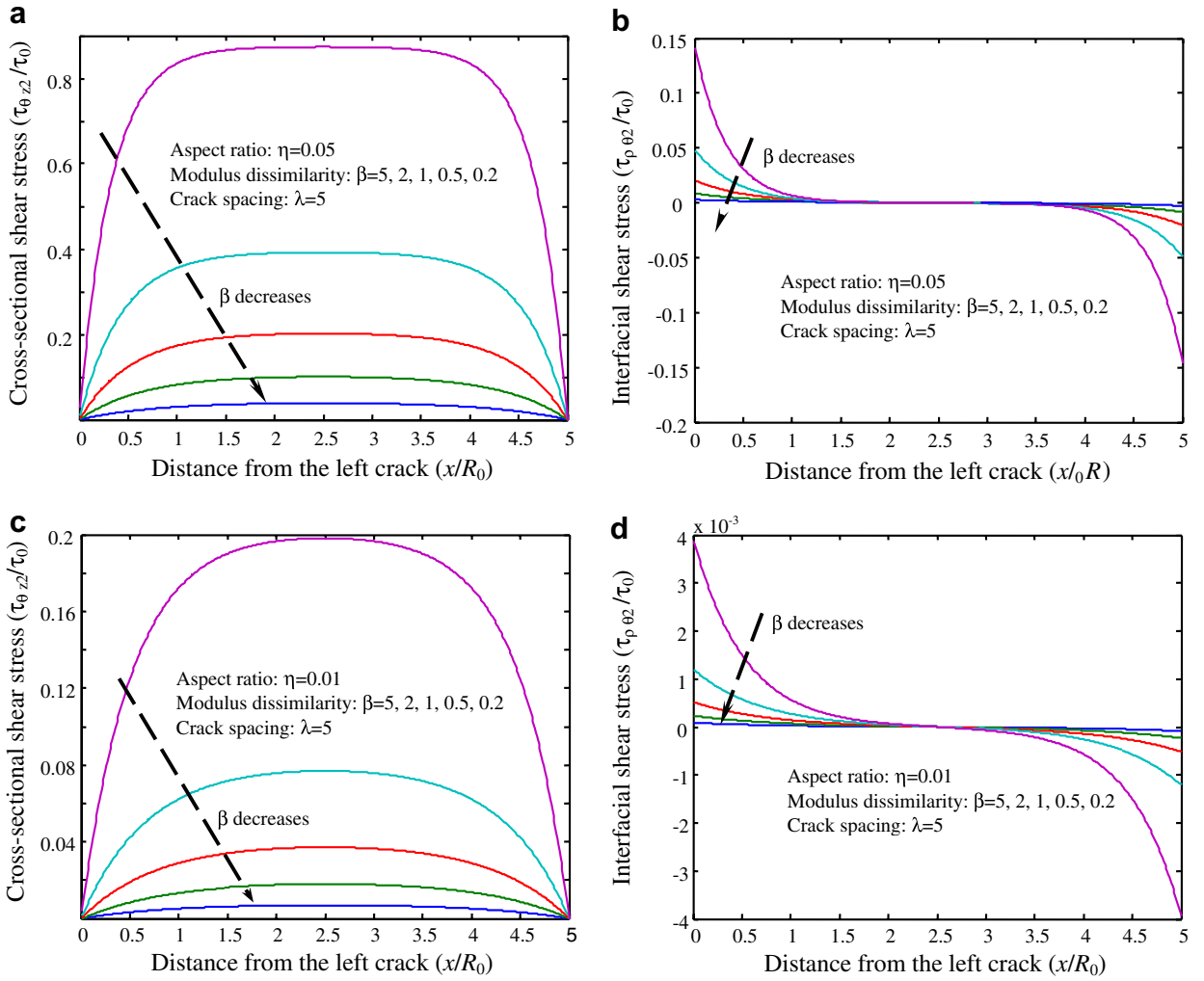

Fig. 4. Interfacial free-edge shear stresses for periodic circumferential cracks in the surface coating layer of a circular torsion bar (dimensionless crack spacing: $\lambda = 5$).

the case of single circumferential cracking, Fig. 3 shows that free-edge effect on the shear stress field is localized within about $1.5R_0$ along axial direction. It also shows that circumferential cracking in relatively stiffer surface coating layers (with higher β-values) tends to induce much higher shear stresses in the coating layers, and in thicker surface coating layers it also tends to induce greater shear stresses. By comparison with the longitudinal shear stresses $\tau_{\theta z2}(1,\xi)/\tau_0$ in coating layers, the interfacial circumferential shear stress $\tau_{\rho\theta 2}(1,\xi)/\tau_0$ are lower, especially in the case of a compliant surface coating layer.

In the case of two adjacent circumferential cracks with varying crack spacing, Figs. 4 and 5 indicate that the shear stress variation is very close to that for a single circumferential crack due to the high localization of the free-edge stresses. As aforementioned in Section 2.2, the actual free-edge stresses near crack tip are singular. However, the present stress solutions provide an efficient method for stress comparison and parameter analysis.

4.2. Critical torque T_c to induce progressive circumferential cracking and resulting crack density in surface coating layers of circular torsion bars

With increasing twisting loads on a circular torsion bar, first circumferential crack may appear once the criterion (3) is satisfied. In this case, the variation of the dimensionless critical torque $T_c/(\pi G_2 G_c R^5)^{1/2}$ vs.

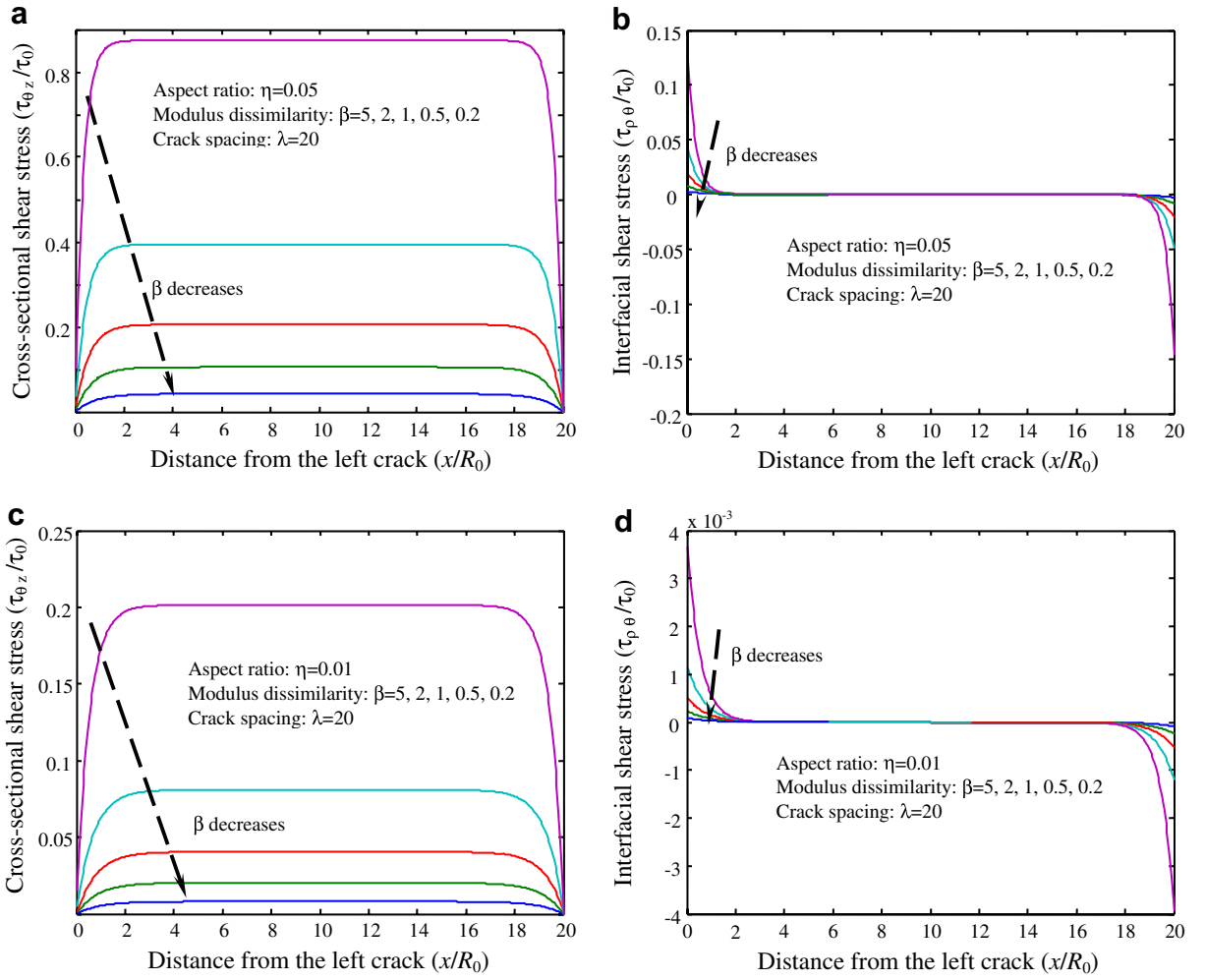

Fig. 5. Interfacial free-edge shear stresses for periodic circumferential crack in the surface coating layer of a circular torsion bar (dimensionless crack spacing: $\lambda = 20$).

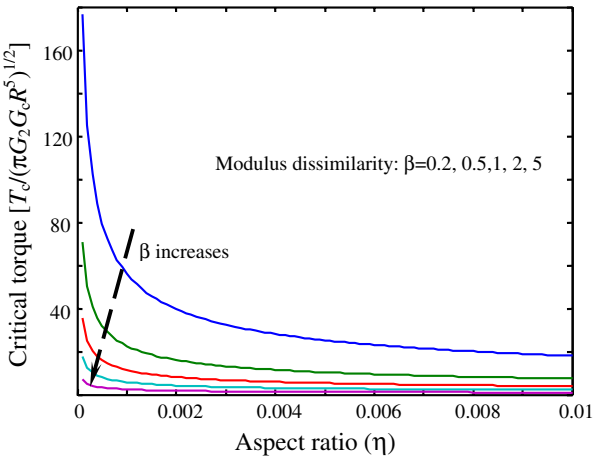

Fig. 6. Variation of the critical torque to induce first circumferential crack vs. the aspect ratio of coating layer for varying index of modulus dissimilarity.

the aspect ratio η at several indices of modulus dissimilarity β is illustrated numerically in Fig. 6. It can be observed that the critical torque decreases rapidly with increasing either the η-value or the β-value, i.e., thicker and stiffer coating layers are more pliable to circumferential cracking.

Now let us consider the progressive circumferential cracking. In this case, the dimensionless progressive cracking density $d = 1/\lambda$ is a function of the dimensionless critical torque $T_c/(\pi G_2 G_c R^5)^{1/2}$, where $\lambda = L/R_0$ is the dimensionless crack spacing. Here the critical torque is understood in the sense of the expected value according to (36), i.e., the expected critical torque to induce the next circumferential crack between two adjacent circumferential cracks with spacing λ. By using the three possibility distributions aforementioned, the variation of the crack density vs. the critical torque is plotted in Fig. 7 for varying η- and β-values. From Fig. 7, it can be found that the three cracking models predict similar density growth trends. The first model (curves with index 1 in Fig. 7) with assumption of next cracking at the mid-point predicts the greatest progressive cracking density, i.e., an aggressive prediction; while the second model with assumption of even cracking predicts the lowest cracking density correspondingly, i.e., a conservative prediction. Furthermore, for given cracking density and aspect ratio, stiffer coating layers with greater β-values result in lower critical torques by comparison with those made of compliant materials. Moreover, the critical torque decreases with increasing the aspect ratio (coating layer thickness) at fixed cracking density. Consequently, when the cracking density tends to

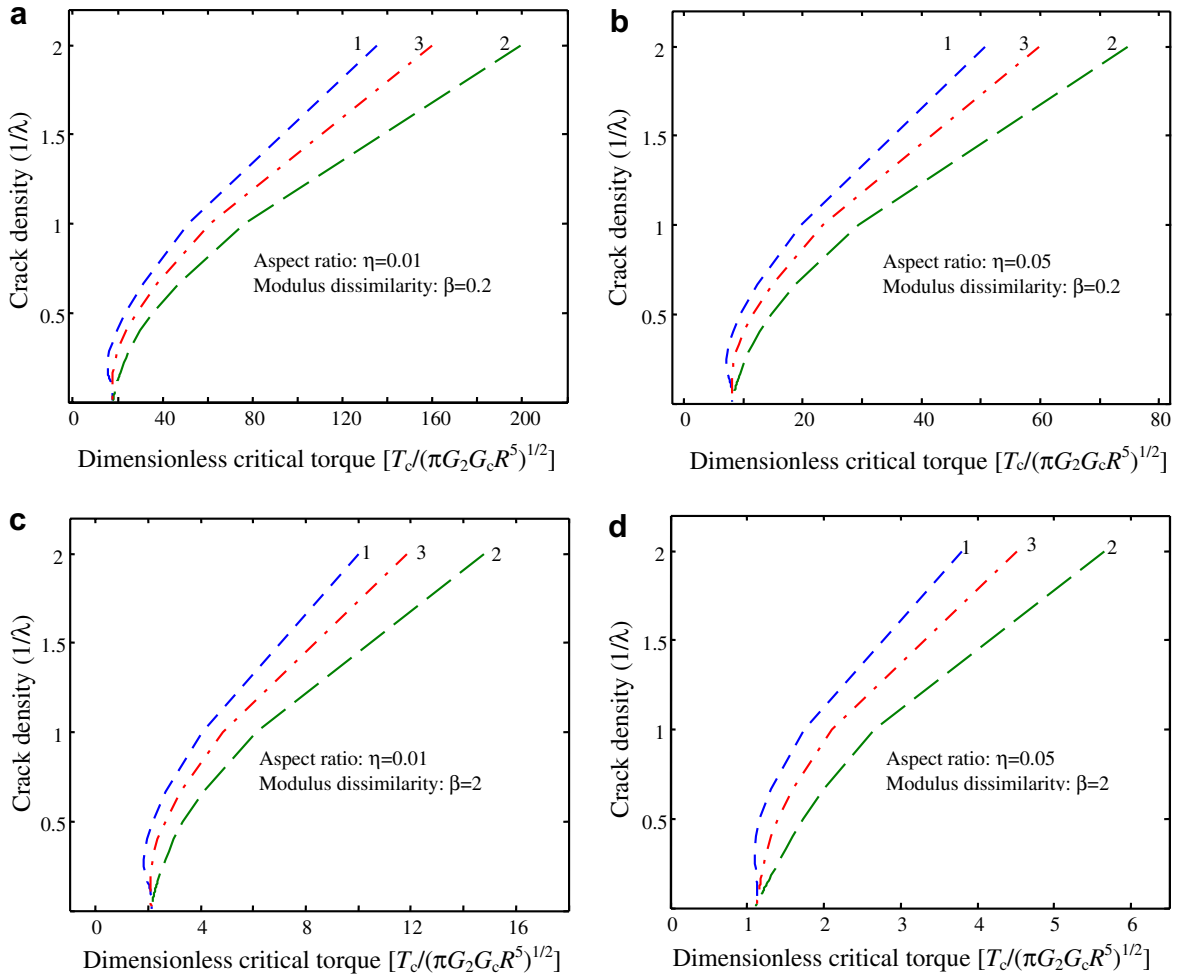

Fig. 7. Variation of the crack density vs. the critical torque to induce the next circumferential crack for several aspect ratios and indices of modulus dissimilarity. Curves with indices 1, 2, and 3 are corresponding to the 1st, 2nd, and 3rd probability distribution models described in Section 3.2, respectively.

zero, i.e., single circumferential cracking, the corresponding critical torques recovers those for single cracks as predicted in relation (35) and illustrated in Fig. 6.

5. Concluding remarks

In this study, within the framework of LEFM, explicit solutions have been developed for the free-edge stresses and progressive cracking of surface coating layers of circular torsion bars. Criteria for progressive cracking of the surface coatings have been established successfully in the sense of conservation of strain energy. This criterion has been demonstrated in predicting the density of progressive cracking in surface coating layers of torsion bars with varying aspect ratio and index of modulus dissimilarity. Effects of external torque, aspect ratio, and elastic properties on the free-edge stress distribution and the density of progressive cracking have been examined. It has been shown that coating layer of compliant materials has much higher critical torque than that of a stiffer one under the condition of same geometries and substrate in inducing given cracking density. Meanwhile, thicker surface coating layers exhibit more pliant to cracking than thin ones. Therefore, the above results can be used to guide the surface coating design and cracking prediction. When the geometries and material properties of the coating system are available, the present model could be used in analyzing the damage mechanism in surface coatings of torsion bars and data reduction of torsion fracture test of surface coatings. In the latter case, the fracture toughness of the surface coating layer can be determined by measuring the crack spacing and using the formulas developed in Section 3.

Acknowledgement

Partial support of this work by the NSF/AFOSR/ARL/ARO was greatly appreciated.

References

Adams, R.D., Peppiatt, N.A., 1977. Stress analysis of adhesive bonded tubular lap joint. J. Adhesion 9, 1–18.
Benthem, J.P., Koitor, W.T., 1973. Asymptotic approximations to crack problems. In: Sih, G.C. (Ed.), Methods of Analysis and Solutions of Crack Problems. Noordhoff International Publishing, Leyden, Netherlands, pp. 131–178.
Chen, D., Cheng, S., 1992. Torsional stress in tubular lap joints. Int. J. Solids Struct. 29, 845–853.
Cox, H.L., 1952. The elasticity and strength of paper and other fibrous materials. Br. J. Phys. 3, 72–79.
Donnet, C., Erdemir, A., 2004. Solid lubricant coatings: recent developments and future trends. Tribol. Lett. 17, 389–397.
Evans, A.G., Mumm, D.R., Hutchinson, J.W., Meier, G.H., Pettit, F.S., 2001. Mechanisms controlling the durability of thermal barrier coatings. Progress Mater. Sci. 46, 505–553.
Faulhaber, S., Mercer, C., Moon, M.W., Hutchinson, J.W., Evans, A.G., 2006. Buckling delamination in compressed multilayers on curved substrates with accompanying ridge cracks. J. Mech. Phys. Solids 54, 1004–1028.
Hu, H.C., 1984. Variational Principles of Theory of Elasticity with Applications. Science Press, Beijing, China.
Hutchinson, J.W., 2001. Delamination of compressed films on curved substrates. J. Mech. Phys. Solids 49, 1847–1864.
Hutchinson, J.W., Suo, Z., 1992. Mixed mode cracking in layered materials. Adv. Appl. Mech. 29, 63–192.
Laws, N., Dvorak, G.J., 1988. Progressive transverse cracking in composite laminates. J. Compos. Mater. 22, 900–916.
Liang, J., Zhang, Z., Prevost, J.H., Suo, Z., 2004. Time-dependent crack behavior in an integrated structure. Int. J. Fracture 125, 335–348.
Mishnaevsky Jr., L.L., Gross, D., 2004. Micromechanisms and mechanics of damage and fracture in thin film/substrate systems. Int. Appl. Mech. 40, 140–155.
Mishnaevsky Jr., L.L., Gross, D., 2005. Deformation and failure in thin films/substrate systems: methods of theoretical analysis. Appl. Mech. Rev. 58, 338–353.
Mittelstedt, C., Becker, W., 2004a. Interlaminar stress concentration in layered structures: part I-a selected survey on the free-edge effect since 1967. J. Compos. Mater. 38, 1037–1062.
Mittelstedt, C., Becker, W., 2004b. Interlaminar stress concentration in layered structures: part I-closed-form analysis of stresses at laminated rectangular wedges with arbitrary non-orthotropic layup. J. Compos. Mater. 38, 1063–1090.
Pipes, R.B., Pagano, N.J., 1970. Interlaminar stresses in composite laminates under uniform axial extension. J. Compos. Mater. 4, 538–548.
Shenoy, V.B., Schwartzman, A.F., Freund, L.B., 2001. Crack patterns in brittle thin films. Int. J. Fracture 109, 29–45.
Singer, I.L., Dvorak, S.D., Wahl, K.J., Scharf, T.W., 2003. Role of third bodies in friction and wear of protective coatings. J. Vac. Sci. Technol. A 21, S232–S240.
Suo, Z.G., Hutchinson, J.W., 1990. Interface crack between two elastic layers. Int. J. Fracture 43, 1–18.
Timoshenko, S., Goodier, J.N., 1951. Theory of Elasticity, second ed. McGraw-Hill, New York.
Vlassak, J.J., 2003. Channel cracking in thin films on substrates of finite thickness. Int. J. Fracture 119–120, 299–323.

Volkersen, O., 1965. Recherches sur la Theorie des Assemblages Colles. Construction Metallique 4, 3–13.
Wang, D.F., Kato, K., 2003a. Nano-scale fatigue wear of carbon nitride coatings: part I – wear properties. J. ASME Tribol. 125, 430–436.
Wang, D.F., Kato, K., 2003b. Nano-scale fatigue wear of carbon nitride coatings: part II – wear mechanisms. ASME J. Tribol. 125, 437–444.
Washizu, K., 1968. Variational Methods in Elasticity and Plasticity. Pergamon Press, New York.
Wu, X.F., Dzenis, Y.A., 2005. Experimental determination of probabilistic edge-delamination strength of a graphite-fiber/epoxy composite. Compos. Struct. 70, 100–108.
Xia, Z.C., Hutchinson, J.W., 2000. Crack patterns in thin films. J. Mech. Phys. Solids 48, 1107–1131.